

Mobile Wireless Network Infrastructure on Demand

Daniel Mox¹, Miguel Calvo-Fullana², Jonathan Fink³, Vijay Kumar¹ and Alejandro Ribeiro²

Abstract—In this work, we introduce *Mobile Wireless Infrastructure on Demand*: a framework for providing wireless connectivity to multi-robot teams via autonomously reconfiguring ad-hoc networks. In many cases, previous multi-agent systems either presumed on the availability of existing communication infrastructure or were required to create a network in addition to completing their objective. Instead our system explicitly assumes the responsibility of creating and sustaining a wireless network capable of satisfying the end-to-end communication requirements of a task team performing an arbitrary objective. To accomplish this goal, we propose a joint optimization framework that alternates between finding optimal network routes to support data flows between the task agents and updating the configuration of the network team to improve performance. We demonstrate our approach in a set of simulations in which a fleet of UAVs provide connectivity to a set of task agents patrolling a perimeter.

I. INTRODUCTION

Wireless networks have become a ubiquitous part of modern life. Today, technologies such as Wi-Fi and cellular networks blanket vast portions of the globe enabling unprecedented access to information. As wireless communication becomes more tightly integrated into everyday life it is increasingly normal to presume on its availability and performance. However, providing widespread wireless connectivity at scale requires tremendous effort both in coordinating large distributed systems and deploying and maintaining costly infrastructure. Indeed, the challenge of delivering wireless connectivity has given rise to a broad spectrum of communication technologies that seek to juggle range, bandwidth, latency, and cost, with no one-size-fits-all solution emerging as of yet. Systems such as Wi-Fi, provide high bandwidth at low cost but are limited in range; on the other hand, far reaching cellular networks require the deployment of expensive fixed infrastructure such as communication towers and base stations.

While areas not covered by fixed infrastructure continue to shrink, there still remain cases where existing wireless networks are unavailable such as underground environments, rural regions, and areas affected by natural disaster. In these scenarios, reliance on existing technology is not possible and

new approaches to providing connectivity must be explored, particularly as it relates to fast deployment of wireless infrastructure. The ability to quickly access information or sustain a communication link can be crucial, especially in disaster recovery and emergency response situations.

With these challenges in mind we introduce a system for delivering *Mobile Wireless Infrastructure on Demand*. Our approach leverages mobile robots equipped with wireless hardware to create and sustain communication networks in dynamic environments. Client users accomplishing tasks requiring communication can connect to the provided network and the network nodes reconfigure and route information to satisfy their demands. While our philosophy would extend to any autonomous robotic platform, due to their versatility, we consider Unmanned Aerial Vehicles (UAVs) equipped with IEEE 802.11 communication hardware which act as an ad-hoc network.

Combining control and communication is a well studied problem in robotics and a considerable amount of research has been devoted to studying the effect communication links and wireless networks have on the ability of agents to coordinate. Many works borrow concepts for algebraic graph theory, specifically properties of the graph Laplacian, in order to reason about the state of a network of agents. Common approaches include maximizing or preserving the algebraic connectivity of a state dependent Laplacian [1]–[6] which can be solved in both a centralized [1]–[3] and decentralized manner [4]–[6]. Wireless channels themselves are extremely difficult to predict and approaches can be categorized by the abstraction they use to model point-to-point communication. Disk models are the simplest and consider all agents within some distance to be in communication range [4], [5], [7], [8]. Other approaches employ a function of the inter-robot distance, often exponential decay, to model the channel [1]–[3], [6], [9]–[11]. More complex models more faithfully honor the uncertainty of predicting wireless links by using probabilistic models to provide both an expected channel rate and associated variance [12]–[16].

In this work we take a similar approach to [17] and more recently [18], which used a probabilistic channel model and robust routing formulation to ensure a team of robots performing some task also satisfies end-to-end communication constraints. In both cases, the task is abstracted as a potential function that is driven to zero as the team accomplishes its objective and a single team of agents responsible for both completing the task and satisfying the associated communication requirements. In this paper we take a different approach by explicitly separating the task and network teams. While many robotic tasks can be reduced

Work supported by ARL DCIST CRA W911NF-17-2-0181 and the Intel Science and Technology Center for Wireless Autonomous Systems.

¹Daniel Mox and Vijay Kumar are with the Mechanical Engineering and Applied Mechanics Department at the University of Pennsylvania, Philadelphia, PA, USA {mox, kumar}@seas.upenn.edu

²Miguel Calvo-Fullana and Alejandro Ribeiro are with the Electrical and Systems Engineering Department at the University of Pennsylvania, Philadelphia, PA, USA {cfullana, aribeiro}@seas.upenn.edu

³Jonathan Fink is with the U.S. Army Research Laboratory, Adelphi, MD, USA {jonathan.r.fink3.civ}@mail.mil

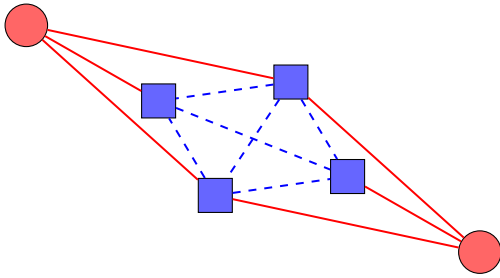


Fig. 1. An example network configuration with task agents as red circles, network agents as blue squares, task-network connections as solid red lines, and inter-network connections as dashed blue lines.

to potential functions (e.g., visiting a goal location) others cannot or must be reasoned about in a more abstract manner. Instead of making limiting assumptions about the type of objective being performed, we define an interface where end-to-end communication rate requirements are provided by the network team. In this way our approach remains task agnostic and applicable to any multi-agent system that can specify its communication requirements.

The rest of this paper is organized as follows: In Section II, we present the main ideas discussed in this work. An overview of the channel model and the abstractions considered is given in Section II-A; Section II-B outlines the network flow model and the routing decisions; In Section II-C, a probabilistic routing approach and the resulting robust routing problem are discussed; and Section II-D details how network reconfiguration is performed. Simulations are discussed in Section III and finally, Section IV closes the paper providing some discussions and future work.

II. PROBLEM INTRODUCTION AND METHODOLOGY

Consider Fig. 1, consisting of a team of mobile robots collaborating to complete a task requiring communication. Instead of creating and sustaining a wireless network in addition to completing their objective, this task team presumes on the ability to communicate while a different group of robots, called the network team, provides the required infrastructure. The network team positions itself in the environment and routes packets such that the task team can go about their objective without concern for the impact of their actions on their ability to communicate. The focus of this paper is on determining network team configuration and routing variables to support the task team's presumption.

More formally, suppose there are p agents in the task team and q agents in network team with $n = p + q$ total agents. \mathcal{I}_T and \mathcal{I}_N represent the ordered set of indices of the task agents and network agents so that $|\mathcal{I}_T| = p$, $|\mathcal{I}_N| = q$, $\mathcal{I}_T \cup \mathcal{I}_N = \{1, 2, \dots, n\}$, and $\mathcal{I}_T \cap \mathcal{I}_N = \emptyset$ (i.e. dual citizenship is not permitted). The position of each agent is given by $x_i \in \mathbb{R}^2$ and the state of the combined teams is $\mathbf{x} = [x_1, x_2, \dots, x_n]^T$. The configuration of the network team is denoted $\mathbf{x}_N = [x_{\mathcal{I}_N(1)}, \dots, x_{\mathcal{I}_N(q)}]^T$ and the task team $\mathbf{x}_T = [x_{\mathcal{I}_T(1)}, \dots, x_{\mathcal{I}_T(p)}]^T$.

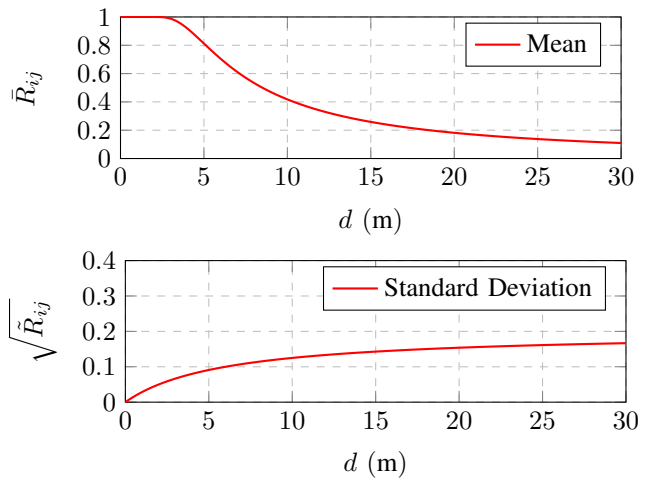


Fig. 2. An example characterization of the rate function $R_{ij}(x_i, x_j)$, where $d = \|x_i - x_j\|$ is the distance between the agents x_i and x_j . The functions plotted are given by equation (1) and (2), with parameters $P_{L_0} = -53$ dBm, $n = 2.52$, $P_{N_0} = -70$ dBm, $a = 0.2$ and $b = 0.6$. This is the characterization used in Section III (Numerical Results).

A. Channel Model

In order to reason about the rate at which packets can be transmitted in a network, it is necessary to predict the state of the wireless channel between pairs of agents. In complex real-world scenarios, this is in itself a challenging task with a large body of research focused on establishing empirical models across a wide range of hardware and environments. While the communication channel observed by the user is dependent of the communication technology used, in this work, our concern is with capturing the dominant characteristics of wireless channels without incurring significant model complexity in addition to remaining somewhat hardware agnostic. To this end, we instead of explicitly modeling the channel, we consider directly the ultimate metric of interest to the task agents, which is the communication rate at which they can reliably transmit. Further, we do not consider an explicit model of the point-to-point achievable rate between two agents. Instead, we distill it to the required properties of the channel rate characterization. Specifically, (i) Increasing the distance between agents diminishes the mean achievable rate and (ii) A decrease in the distance between agents results in an increase on the confidence of the receive rate.

More formally, we consider a normalized rate function $R_{ij}(x_i, x_j) \in [0, 1]$ between two agents located at positions x_i and x_j . This rate function is a random variable representing how much available transmission rate a point-to-point link has, and which depends on the randomness of the communication channel. For the purposes of analysis, we resort to a statistical characterization of these rates, denoting by \bar{R}_{ij} and $\tilde{R}_{ij}(x_i, x_j)$, their mean and variance, respectively. Specifically, we consider the following characterization during the numerical results, which is also plotted

in Figure 2,

$$\bar{R}_{ij}(x_i, x_j) = \text{erf} \left(\sqrt{\frac{P_{L_0}}{P_{N_0}}} \|x_i - x_j\|^{-n} \right), \quad (1)$$

$$\tilde{R}_{ij}(x_i, x_j) = \frac{a \|x_i - x_j\|}{b + \|x_i - x_j\|}, \quad (2)$$

where $\text{erf}(x) = \frac{2}{\sqrt{\pi}} \int_{-x}^x e^{-t^2} dt$ is the Gauss error function, P_{L_0} is the transmit power, n is the decay rate and P_{N_0} is the noise at the receiver, and $a = 0.2$ and $b = 0.6$ are decay parameters. This model is formed by composing generic models for received signal strength and bit error rate to obtain a channel rate estimate [19].

B. Network Flows

As the task team moves to accomplish its objective, data is transmitted between source nodes and destination node(s) in the task team via the network team. These flows of information are indexed by $k \in \{1, 2, \dots, K\}$ with the set of source and destination nodes for flow k given by $S_k, D_k \in \mathcal{I}_T$, respectively. As an example, in a collaborative mapping task flow k might refer to the regular transmission of newly gathered observations of the environment from a foraging task agent i ($S_k = \{i\}$) to the rest of the team ($D_k = \mathcal{I}_T \setminus i$). Each flow requires a certain minimum communication rate in order to be transmitted successfully. The required minimum rate at source node i for flow k is given by m_i^k . For network team nodes that do not contribute new packets to the network but simply act as relays, $m_i^k = 0$.

Data packets are relayed through the network according to routing variables $\alpha_{ij}^k \in [0, 1]$ which represent the probability or the fraction of an arbitrary time step node i spends transmitting data associated with flow k to node j . The set of all routing variables is denoted by α . Routing variables must satisfy $\sum_{j,k} \alpha_{ij}^k \leq 1$ as well as $\sum_{i,k} \alpha_{ij}^k \leq 1$, which are the upper bound on channel transmission and receiver usage during a time step. Finally, task agents access the network as clients; if task agent i is the source of flow k then $\alpha_{ij}^k = 0 \forall j$ (i.e. data is not returned to the source node) and similarly if agent j is the destination then $\alpha_{ij}^k = 0 \forall i$ (i.e., destinations nodes don't rebroadcast data once it has been received). These in and out of node flow equations are given by the following difference equations

$$b_i^k(\alpha, \mathbf{x}) = \sum_{j=1}^n \alpha_{ij}^k R_{ij}(x_i, x_j) - \sum_{j=1}^n \alpha_{ji}^k R_{ji}(x_j, x_i), \quad (3)$$

where, since the rates $R_{ij}(x_i, x_j)$ are random variables, we resort to a statistical representation, and the mean and variance of the flow equations are given by

$$\bar{b}_i^k(\alpha, \mathbf{x}) = \sum_{j=1}^n \alpha_{ij}^k \bar{R}_{ij}(x_i, x_j) - \sum_{j=1}^n \alpha_{ji}^k \bar{R}_{ji}(x_j, x_i), \quad (4)$$

$$\tilde{b}_i^k(\alpha, \mathbf{x}) = \sum_{j=1}^n (\alpha_{ij}^k)^2 \tilde{R}_{ij}(x_i, x_j) + \sum_{j=1}^n (\alpha_{ji}^k)^2 \tilde{R}_{ji}(x_j, x_i), \quad (5)$$

where we denote by \bar{b}_i^k the expected rate margin of node i for flow k , $i \in S_k \cup \mathcal{I}_N$ and by \tilde{b}_i^k the confidence in the expected rate margin. In order for packets to be routed through the network and delivered as required it is sufficient to ensure the flow of data into and out of each node remains balanced, preventing unbounded accumulation of packets at any node leading to queue overflow. Thus, the flow of data into and out of a node must satisfy the stability condition

$$\bar{b}_i^k \geq m_i^k, \quad (6)$$

where i assumes the same values as before.

C. Probabilistic Routing

Since the rate margin b_i^k is a random variable [cf. expression (3)], it can only be satisfied in a probabilistic sense. Namely,

$$\mathbb{P} [\bar{b}_i^k(\alpha, \mathbf{x}) \geq m_i^k] \geq 1 - \epsilon_k, \quad (7)$$

where ϵ is the risk of the constraint being unsatisfied and $1 - \epsilon$ is the confidence with which the constraint is met. Thus, the pair $(m_i^k, 1 - \epsilon_k)$ forms the communication rate specification requested by the user. Specifically, the i -th user demands for its k -th flow a communication mean communication rate of m_i^k with confidence $1 - \epsilon_k$.

For a wide class of probability distributions expression (7) can be satisfied using Chebyshev's inequality. However, tighter bounds can be achieved if the distribution is known. In the following, we assume that the rate margin b_i^k is normally distributed and equation (5) can then be expressed as

$$\frac{\bar{b}_i^k(\alpha, \mathbf{x}) - m_i^k}{\sqrt{\tilde{b}_i^k(\alpha, \mathbf{x})}} \geq \Phi^{-1}(1 - \epsilon_k), \quad (8)$$

where $\Phi^{-1}(\cdot)$ is the inverse normal cumulative distribution function. Now, we intend to find, given team configuration \mathbf{x} , the set of routing variables α which satisfy equation 8. However, there may be many sets of routing variables α that satisfy equation (7). We are interested in those that do so with the highest margin. Thus, a nonnegative slack variable s is introduced and the robust routing problem is posed as follows

$$\text{maximize}_{\alpha \in \mathcal{A}, s \geq 0} s \quad (9a)$$

$$\text{subject to} \quad \frac{\bar{b}_i^k(\alpha, \mathbf{x}) - m_i^k - s}{\sqrt{\tilde{b}_i^k(\alpha, \mathbf{x})}} \geq \Phi^{-1}(1 - \epsilon_k) \quad (9b)$$

for all i and k , and where \mathcal{A} is the set of implicit routing constraints, composed of $\alpha_{ij}^k \in [0, 1]$ (routing variables are a probability), $\sum_{j,k} \alpha_{ij}^k \leq 1$ (bounded channel transmission), $\sum_{j,k} \alpha_{ij}^k \leq 1$ (bounded receiver usage), $\alpha_{ij}^k = 0$ for $i \in \mathcal{I}_T \setminus S_k$ (destination nodes don't transmit), $j \in \mathcal{I}_T \setminus D_k$ (packets are not returned to the source node). Following the approach in [17], the optimization problem (9) can be posed as a Second Order Cone Problem (SOCP) and a solution obtained using an available convex solver. Note that the network team configuration \mathbf{x}_N is not one of the optimization variables; The solution to the optimization problem (9)

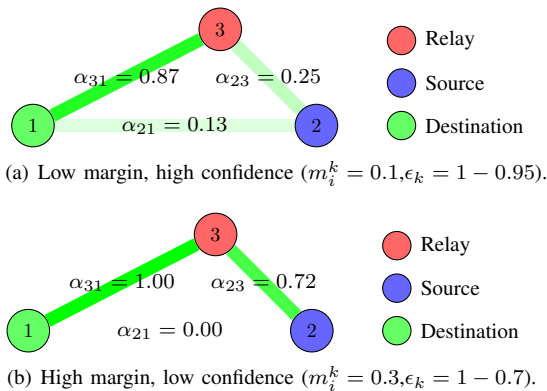


Fig. 3. Optimal solutions of the robust routing problem for different margin and confidence requirements. High margin with low confidence prioritizes the strongest links while low margin with high confidence splits traffic among the routes.

supplies valid robust routing variables given a feasible team state \mathbf{x} .

Increasing the slack s is equivalent to increasing the margin with which the probability constraints in equation (7) are satisfied. This can be accomplished by increasing the expected value \bar{b}_i^k , by prioritizing channels with high expected rate \bar{R}_{ij} , and/or decreasing the variance \tilde{b}_i^k , by splitting routes between multiple nodes. For flows with high requirement m_i^k and low confidence $1 - \epsilon_k$, packets flow mainly through high rate channels; for flows with low requirement and high confidence, packets are split along multiple routes (This is illustrated in Figure 3). Thus, the solution to the robust routing problem (9) prioritizes end-to-end performance while seeking to be robust to point-to-point failures, accounting for model uncertainty.

D. Network Reconfiguration

Solving the robust routing problem (9) allows us to find the optimal routing variables α_{ij}^k given a network team configuration \mathbf{x}_N and task team configuration \mathbf{x}_T . Now, we are interested in finding the network team configurations \mathbf{x}_N that satisfy the constraints of problem (9) (recall only the positions of the network agents can be controlled). As the task agents move, the network agents must also adjust their positions to ensure that the communication requirements are met. Unfortunately, the rate margins in equation (4) are non-convex in \mathbf{x} , precluding some kind of joint optimization of α and \mathbf{x}_N directly. While the gradient of slack s with respect to the team configuration could be computed from the rate estimation function presented in Section II-A, we are interested in developing a system that works for a family of rate functions meeting the requirements outlined in Section II-A. In other words, we assume that a rate function can be efficiently queried for $\bar{R}_{ij}, \tilde{R}_{ij}$ but do not make further restrictions to its form (e.g., that it be differentiable).

Similar approaches solve this problem by using a sampling based gradient approximation to drive the team away from configurations that violate the communication requirements all while minimizing a task potential function [17]. In our

Algorithm 1 Local controller

Input: $\mathbf{x}_N, \mathbf{x}_T, \mathbf{x}_N^*$

Output: \mathbf{x}_N^*

- 1: $\alpha = \text{SOCP}([\mathbf{x}_T, \mathbf{x}_N])$
 - 2: $\alpha^* = \text{SOCP}([\mathbf{x}_T, \mathbf{x}_N^*])$
 - 3: $v^* = \nu(\alpha^*, [\mathbf{x}_T, \mathbf{x}_N^*])$
 - 4: **for** $i = 0$ to `max_it` **do**
 - 5: $x_p = \text{draw_sample}(\mathbf{x}_N)$
 - 6: $v_p = \nu(\alpha, [\mathbf{x}_T, \mathbf{x}_p])$
 - 7: **if** $v_p > v^*$ **then**
 - 8: $\mathbf{x}_N^* = \mathbf{x}_p$
 - 9: **end if**
 - 10: **end for**
 - 11: **return** \mathbf{x}_N^*, α
-

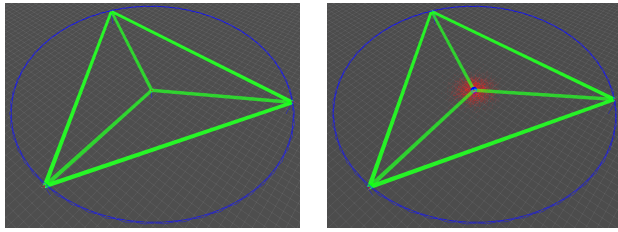
case, the network team's singular focus is to improve the degree to which the node margin constraints of equations (4) are met (i.e. adjusting \mathbf{x}_N to further increase the slack s in the robust routing problem (9)). While one method for doing so is to follow an approximate gradient, a more direct approach is to leverage the same samples to search for configurations that improve on the solution of (9).

Given a solution to the robust routing problem, the constraint closest to being violated can be computed by plugging the solution into equation (8) and selecting the minimum value

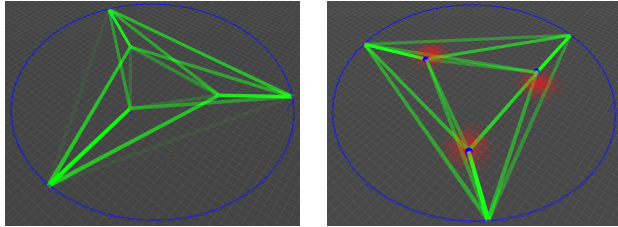
$$\nu(\alpha, \mathbf{x}) = \min_{i,k} \left[\frac{\bar{b}_i^k(\alpha, \mathbf{x}) - m_i^k}{\sqrt{\tilde{b}_i^k(\alpha, \mathbf{x})}} - \Phi^{-1}(1 - \epsilon_k) \right], \quad (10)$$

where $\nu(\alpha, \mathbf{x}) \geq 0$ for all feasible configurations. Furthermore, the greater $\nu(\alpha, \mathbf{x})$ becomes, the more room the slack s has to grow in (9). Assuming solutions to the optimization problem (9) do not change significantly over short distances, equation (10) provides a method for checking if a neighboring location results in a better network configuration (one with higher slack) much more efficiently than resolving the SOCP. This insight forms the foundation of local control scheme outlined in Algorithm 1.

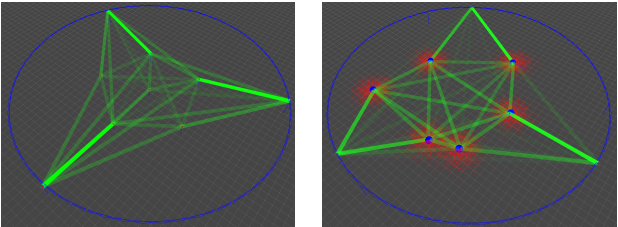
Algorithm 1 is designed to be run in a continuous loop where `max_it` is selected to respect the real-time requirements of the system. In Steps 1 and 2, the set of optimal routing variables with respect to the current team configuration, α , and with respect to the current task team and optimal network team configuration, α^* , are computed by solving the robust routing optimization problem (9) ($\text{SOCP}(\cdot)$ returns the routing variables of the associated solution). It is necessary to recompute α^* as the task team may have moved since the last call even though \mathbf{x}_N^* remains constant. Step 3 finds the constraint closest to being violated for the current optimal configuration, which serves as the benchmark candidate configurations must beat in the local search performed in Steps 4-10. The function `draw_sample`(\mathbf{x}_N) returns a collision free ($\|x_i - x_j\| > d_c$ for $i, j \in \{1, \dots, n\}$ and $i \neq j$, given some distance d_c) network team configuration in the neighborhood of \mathbf{x}_N drawn from some probability



(a) Resulting configurations with $q = 1$ network agent.



(b) Resulting configurations with $q = 3$ network agents.



(c) Resulting configurations with $q = 6$ network agents.

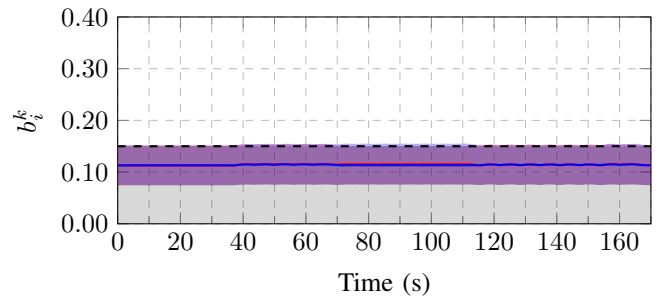
Fig. 4. Representative network configurations for the team of static agents used as the baseline (left) and the team of dynamics agents running our proposed algorithm (right) for the patrol scenario with $p = 4$ task agents tracing the perimeter of a circle with a radius of 20 m. The size of the network team is $q = 1$ in row (a) $q = 3$ in row (b) and $q = 6$ in row (c)

distribution. Then if the candidate configuration \mathbf{x}_p is found to be better, the optimal configuration is updated and the search continues. Since \mathbf{x}_N^* persists across iterations, Algorithm 1 drives the network team towards locally optimal network configurations.

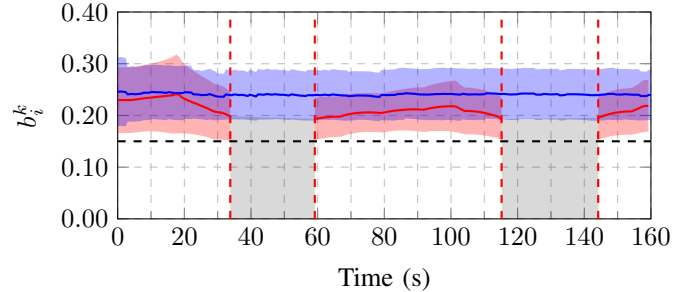
III. NUMERICAL RESULTS

In order to verify our proposed algorithm, we implemented our system in ROS [20] and performed a suite of simulations using Gazebo [21]. We considered a scenario where a team of three task agents patrolling a perimeter desired to exchange information; however, due to their relative distance their communication requirements could not be satisfied by directly broadcasting to one another. Thus, we deployed a team of network agents to act as relays, ensuring critical information from the patrolling agents were delivered to the others.

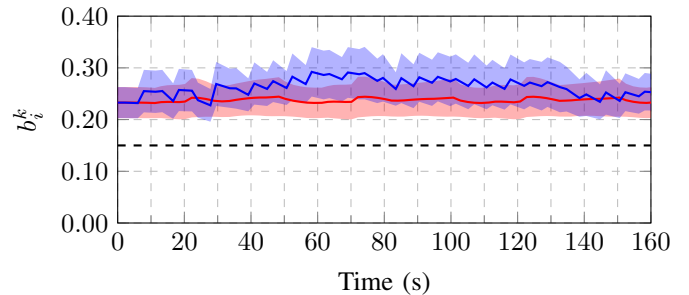
In this scenario, the communication requirements of the task team were modeled as three flows: agent 1 to agents 2,3; agent 2 to agents 1,3; and agent 3 to agents 1,2. For each flow the required margin was $m_i^k = 0.15$ with a confidence of $1 - \epsilon_k = 0.7$. The channel parameters in question were chosen for IEEE 802.11 [16] and the exact values are listed in Fig. 2.



(a) Resulting rates with $q = 1$ network agent. Both the fixed and the dynamic team configurations are the same and cannot support the demanded rate specification.



(b) Resulting rates with $q = 3$ network agents. The dynamic team successfully supports the demands while the fixed team sporadically fails to do so



(c) Resulting rates with $q = 6$ network agents. Both the fixed configuration and the dynamic configuration can support the demand rate specification with the dynamic team performing better on average

Fig. 5. Average rate margin at the source node for $p = 3$ task agents requiring a rate margin of $m_i^k = 0.15$ with confidence $1 - \epsilon = 0.7$. The network team ranges in with $q = \{1, 3, 6\}$ in the rows (a), (b), and (c) respectively. The average rate margin of the fixed network team is shown in red and the dynamic team executing our local controller in blue. The $1 - \epsilon = 0.7$ confidence bound for each margin is shown as the filled in region.

As our system does not directly prescribe the number of agents required to satisfy the task requirements, we conducted simulations with network teams of 1, 3, and 6 agents running our local controller. As a point of comparison, we also conducted the same simulations with a fixed network team deployed in a configuration to best cover the task space but not allowed to move with the task agents. The fixed network configurations are shown in the left column of images in Fig. 4 and representative configurations of the mobile network team in action are shown in the right column. Green lines denote active network links with the opacity

indicating the corresponding routing variable with opaque links being utilized more heavily than transparent ones.

The performance of the network team in each scenario was measured as the average of the rate margins at the source nodes: b_1^1 , b_2^2 , and b_3^3 . Recall that the optimization problem (9) either finds a feasible set of routing variables for all flows or is infeasible; thus, the performance of the system can be effectively judged by considering the three rate margins together. The average rate margin of the fixed and dynamic teams are shown in Fig. 5 where the solid lines represent the average rate margin at the source and the $1 - \epsilon_k = 0.70$ confidence bounds are shown as the filled in regions.

Fig. 4(a) which shows the configuration for a single network agent. In this case, the fixed configuration and dynamic configurations coincide at the center of the circle. Whenever that the dynamic system is started at a different position, the algorithm pulls the agent to the center, which is the optimal configuration and evenly distributes traffic across the links. In the single agent case the system cannot satisfy the task requirements of $m_i^k = 0.15$ and $1 - \epsilon = 0.7$. As shown in Fig. 5(a), the best rate that can be provided (and it is the same for both our algorithm and the baseline) is only around ~ 0.12 .

For three agents, the fixed configuration was chosen to be a triangle centered in the circle as seen in Fig. 4(b). While this fixed triangle configuration performed well when the task team was aligned with it, the average rate margin suffered as the task team moved away and ultimately was unable to satisfy the communication requirements over the entire patrol trajectory as illustrated in the grey regions of Fig. 5(b). On the contrary, the three agent network team running our local controller converged to a triangle that rotated along with the patrol agents (Fig. 4(b)) providing consistent communication throughout the duration of the task.

Finally, a deployment with six network agents is shown in Fig. 4(c). In this case the best fixed team configuration is not immediately obvious. We opted for a space filling pentagon with an agent at the center to cover the interior of the circle. In this case as the number of agents increases their relative positioning becomes less crucial; while the dynamic network team performed better on average, the fixed team was also able to support the required rate over the duration of the patrol as evidenced in Fig. 5(c).

IV. CONCLUSIONS AND FUTURE WORK

In this paper, we have introduced an architecture for providing mobile wireless network infrastructure. A key component in our approach is the definition of an interface through which task agents demand a certain quality of service out of the network, that is then provided to them by the network agents. This interface maintains our system task-agnostic and allows the task team to perform an arbitrary task under the assumption of available communication while the network team provides the wireless network infrastructure.

In ongoing future work, we are pursuing the deployment of a fleet of autonomous UAVs with IEEE 802.11 communication hardware implementing our proposed algorithms. We

intend to demonstrate the viability of using our approach to provide mobile wireless network infrastructure on demand.

REFERENCES

- [1] Y. Kim and M. Mesbahi, "On maximizing the second smallest eigenvalue of a state-dependent graph laplacian," in *Proceedings of the 2005, American Control Conference, 2005.*, pp. 99–103, IEEE, 2005.
- [2] E. Stump, A. Jadbabaie, and V. Kumar, "Connectivity management in mobile robot teams," in *2008 IEEE international conference on robotics and automation*, pp. 1525–1530, IEEE, 2008.
- [3] M. M. Zavlanos and G. J. Pappas, "Potential fields for maintaining connectivity of mobile networks," *IEEE Transactions on robotics*, vol. 23, no. 4, pp. 812–816, 2007.
- [4] M. M. Zavlanos and G. J. Pappas, "Distributed connectivity control of mobile networks," *IEEE Transactions on Robotics*, vol. 24, no. 6, pp. 1416–1428, 2008.
- [5] M. Ji and M. Egerstedt, "Distributed coordination control of multi-agent systems while preserving connectedness," *IEEE Transactions on Robotics*, vol. 23, no. 4, pp. 693–703, 2007.
- [6] M. C. De Gennaro and A. Jadbabaie, "Decentralized control of connectivity for multi-agent systems," in *Proceedings of the 45th IEEE Conference on Decision and Control*, pp. 3628–3633, IEEE, 2006.
- [7] D. P. Spanos and R. M. Murray, "Motion planning with wireless network constraints," in *Proceedings of the 2005, American Control Conference, 2005.*, pp. 87–92, IEEE, 2005.
- [8] G. Notarstefano, K. Savla, F. Bullo, and A. Jadbabaie, "Maintaining limited-range connectivity among second-order agents," in *2006 American control conference*, pp. 6–pp, IEEE, 2006.
- [9] M. Schuresko and J. Cortés, "Distributed motion constraints for algebraic connectivity of robotic networks," *Journal of Intelligent and Robotic Systems*, vol. 56, no. 1-2, pp. 99–126, 2009.
- [10] M. M. Zavlanos, A. Ribeiro, and G. J. Pappas, "Network integrity in mobile robotic networks," *IEEE Transactions on Automatic Control*, vol. 58, no. 1, pp. 3–18, 2012.
- [11] O. Tekdas, W. Yang, and V. Isler, "Robotic routers: Algorithms and implementation," *The International Journal of Robotics Research*, vol. 29, no. 1, pp. 110–126, 2010.
- [12] Y. Mostofi, "Communication-aware motion planning in fading environments," in *2008 IEEE International Conference on Robotics and Automation*, pp. 3169–3174, IEEE, 2008.
- [13] Y. Mostofi, A. Gonzalez-Ruiz, A. Gaffarkhah, and D. Li, "Characterization and modeling of wireless channels for networked robotic and control systems—a comprehensive overview," in *2009 IEEE/RSJ International Conference on Intelligent Robots and Systems*, pp. 4849–4854, IEEE, 2009.
- [14] Y. Yan and Y. Mostofi, "Robotic router formation in realistic communication environments," *IEEE Transactions on Robotics*, vol. 28, no. 4, pp. 810–827, 2012.
- [15] J. Fink, A. Ribeiro, and V. Kumar, "Robust control of mobility and communications in autonomous robot teams," *IEEE Access*, vol. 1, pp. 290–309, 2013.
- [16] J. Fink, "Communication for teams of networked robots," 2011.
- [17] J. Fink, A. Ribeiro, and V. Kumar, "Robust control for mobility and wireless communication in cyber-physical systems with application to robot teams," *Proceedings of the IEEE*, vol. 100, no. 1, pp. 164–178, 2011.
- [18] J. Stephan, J. Fink, V. Kumar, and A. Ribeiro, "Concurrent control of mobility and communication in multirobot systems," *IEEE Transactions on Robotics*, vol. 33, no. 5, pp. 1248–1254, 2017.
- [19] R. Shorey, A. Ananda, M. C. Chan, and W. T. Ooi, *Mobile, wireless, and sensor networks: technology, applications, and future directions*. John Wiley & Sons, 2006.
- [20] "Robot Operating System (ROS)." <https://www.ros.org/>.
- [21] "Gazebo Simulator." <http://gazebo.org/>.